A THEORETICAL EARTHQUAKE MODEL TO COMPLEMENT EMPIRICAL STUDIES OF STRONG GROUND MOTION ATTENUATION

Jean Savy (I) and C. Allin Cornell (II)

SUMMARY

A geophysical model of earthquake ground motion is presented with an analysis of its behavior. The motion is created by a shear dislocation of the earth spreading over independent patches with random source parameters. It is found that the size of these patches is a critical factor in assessing the peak acceleration at a given site. The rise time in the dislocation function is also predominant but appears to be strongly correlated with the patch length. Intended to be used as a complement to actual data in attenuation studies, this model will also be helpful in cases where only general behaviors or relative values are necessary.

INTRODUCTION

The sparsity of strong motion earthquake records and the relative clustering of the available data within limited ranges of distances and magnitudes have made it difficult to determine attenuation laws with accuracy empirically. For instance, a lack of data for medium to high magnitudes at distances such as a few kilometers is typical of the data sets. Also typical is a large scatter. Consequently it is virtually impossible to derive attenuation formulas valid for wide ranges of magnitudes or distances. One approach to this problem has been to limit the studies to a relatively narrow range of distances and/or magnitudes and also in some cases to a given type of source mechanisms and geologic environments. (See for instance Reference 7).

A major source of difficulty comes from the complex nature of earthquakes and the large number of variables involved. Such variables as azimuthal direction, size of the fault rupture, nature of the medium through which the waves propagate, rupturing process by discrete patches, existence of high resistance segments along the fault plane are a few of the variables studied in recent years, and most of those parameters are not directly observable. In this paper, an improvement of the geophysical model of ground motion presented by Savy (1979) is used as a tool for understanding the effect of some of these variables. The preliminary results presented here are part of a more complete sensitivity analysis.

Description of the model. It is now accepted that shallow and intermediate earthquakes are caused by a shear break along a slip surface. In the present model the fault rupture is represented by an assemblage of patches

(I) Research Associate, MIT Department of Civil Engineering, Cambridge, Massachusetts, USA.

(II) Professor, MIT Department of Civil Engineering, Cambridge, Massachusetts, USA.

random in shapes and size. The actual rupture development among the patches forms a process similar to a directed random walk in which the mean rupture front spreads out from a specific focal point. A Haskell dislocation is assumed (Haskell 1964, 1966) for each patch and the corresponding acceleration at a given site is computed by assuming a full space elastic homogeneous medium. Only the direct P and S body waves are considered and the effect of the free surface is approximately taken into account by taking twice the full space solution (Anderson 1976). A ramp function with rise time computed independently from the size of each patch is used for the dislocation function. The analytical solution for Fourier Transform of the acceleration at the site, created by the rupture of the j^{th} patch is given by the vectorial equation:

$$[\Gamma_j(\omega)] = \frac{2M_j}{4\pi\rho r_j} e^{-i\omega\left(\frac{\tau_j}{2} + t_j\right)} \frac{\sin \omega\tau_j/2}{\omega\tau_j/2} [G_j]\ C(\omega) \qquad (1)$$

in which: M is the seismic moment, τ is the rise time, t is the first dislocation time, ρ is the mass density, r is the distance from the patch to the site, $C(\omega)$ is a causal filter which includes the material damping and $[G_j]$ is the three component vector which includes the radiation pattern correction and the participation of the P and S waves for the near and far field. For the strike slip case where the site is far enough from all segments of the fault so that the far field solution is applicable, in the standard spherical system of coordinates, $[G_j]$ is given by:

$$[G_j] = \begin{vmatrix} G_r \\ G_\theta \\ G_\phi \end{vmatrix} = \begin{vmatrix} \frac{\sin^2\theta \sin 2\phi}{a^3} G_j^{(a)} & \text{(P-wave)} \\ \frac{\sin 2\theta \sin 2\phi}{2b^3} G_j^{(b)} & \text{(S-wave)} \\ \frac{\sin\theta \cos 2\phi}{b^3} G_j^{(b)} & \text{(S-wave)} \end{vmatrix} \qquad (2)$$

and

$$G_j^c = e^{\left(\frac{-iwr_j}{c} + T_L^c - T_w^c\right)} \frac{\sin \omega T_w^c}{\omega T_w^c} \frac{\sin \omega T_L^c}{\omega T_L^c}$$

$$T_L^c = \frac{L}{2}\left(\frac{1}{v} - \frac{\sin\theta \cos\phi}{c}\right), \quad T_w^c = \frac{w}{2}\frac{\cos\theta}{c}$$

in which c = either a or b, the P and S wave velocities, respectively. For different rupture configurations, such as dip slip, the functions T_L^c and T_w^c may take other forms, and for the solution in the near field some complex correction terms are introduced which essentially modify the phase function.

The Fourier Transform of the acceleration at the site due to the rupture of all the patches is then computed point by point for each frequency by complex addition of all the patches' Fourier Transforms. The result is then used directly as a frequency-domain description or, after computing the inverse function, as the acceleration time history. For some statistical analysis however, the Power Spectral Density (PSD) is computed by averaging the square of the Fourier Transform divided by the duration of motion over an ensemble of simulations. The mean square acceleration is then computed by integration of the PSD.

Analysis and Results. This preliminary sensitivity analysis was divided into three groups of investigations in order to study on the one hand the characteristics of the analytical solution and on the other hand the overall behavior of the model. For all cases a simple geometry is used where the site is located at a distance of 8km on a normal bisecting the fault trace. No attempt has been made yet to look at directional effects or even at the possible variation on the velocity of propagation of the waves, the rupture front, or the material properties.

In the first group of investigations acceleration at the site was computed for the rupture of a single element (one patch). The influence of the size of the element with constant rise-time, the influence of the rise-time with constant seismic moment areal density, the influence of the seismic moment and finally the influence of the size and rise-time combined were investigated.

In the second group a more realistic case was considered. The motion was calculated for a $(6x3)km^2$ rupture fault corresponding roughly to a magnitude 5.5 event with possible multi patch rupture. Our main concern was to study the variation of the average peak acceleration from 5 synthetic records versus the average length of the patches (coherence length). Then this operation was repeated for a $(19x9.5)km^2$ rupture corresponding to a magnitude 6.5 event, but owing to computer cost only one synthetic record was computed for each average coherence length.

In the third group the PSD was computed by generating an ensemble of at least 20 synthetic Fourier Transforms of acceleration for two cases:

(a) for three sizes of earthquakes (seismic moment 2, 63 and 2000 10^{17} m.N corresponding to magnitudes 5.5, 6.5 and 7.5) (See Table III(a))

(b) for three distances 6, 8 and 12 km and an earthquake of seismic moment 2 10^{17} m.N corresponding to magnitude 5.5, the size of which was (6x3)km x km. (See Table III(b)).

In both those cases, the coherence length associated with the seismic moments were subjectively chosen as 2, 6 and 20 km for 2, 63 and 2000 10^{17} m.N respectively.

The results of this analysis are presented here essentially in terms of effect of the different parameters on the peak or RMS acceleration. Certainly other parameters such as the corner frequency, high frequency levels, overall shape of the spectra and total duration are at the present time being considered as well.

Table I summarizes the results of the first group. Not shown here are results showing, as expected from equation (1), that the peak acceleration for a single element is proportional to the seismic moment. In all cases, the corner frequency increased with decreasing size or decreasing rise time, or both. Also expected was the effect of changing the rise time, since it appears in a sinc function in equation 1, that is, the peak acceleration is roughly inversely proportional to the rise time and therefore the corner frequency increases with the peak acceleration.

The results of the analyses of the second group are presented in the Table II. The model appears to be very sensitive to the choice of coherence length, $\bar{\ell}$, especially if one selects a high coherence length. In that case the peak acceleration becomes unrealistically small. This conclusion applies in particular to the results of the third group of Table III(a) where a too large $\bar{\ell}$ in the case of the medium and the large earthquakes led to much too small values of the RMS acceleration. Another point of interest lies in the fact that ruptures which occur on fault planes with abnormally small coherence length will generate very high peak accelerations. This investigation tends to show that there would be a positive correlation between the size of the earthquake (its seismic moment) and the coherence length with earthquakes in the 5-6 (local) magnitude ranges having $\bar{\ell}$ in the 1-3 km and earthquakes in the 6.5-7.5 magnitude ranges having $\bar{\ell}$ in the 5-15 km range. These conclusions are also consistent with inferences by others, for example, the San Fernanco 1971 earthquake of magnitude $M_b = 6.2$, and seismic moment $M_0 = 1.2\ 10^{19}$ m.N had $\bar{\ell} = 2$-5 km (Shakal 1979), Parkefield 1966 ($M_b = 5.3$, $M_0 = 5.5\ 10^{18}$ m.N) had $\bar{\ell} = 1$-3 km and Fort Tejon 1857 ($M_0 = 2.25\ 10^{22}$ m.N) had $\bar{\ell} = 15$ km (Aki 1979).

Figure 1 shows the evolution of the record shape as the coherence length decreases and Figure 2 represents the 3 PSD corresponding to the results of Table III(a). Note that despite an increase in seismic moment the (relatively) high frequency content decreases when the associated increase in coherence is also considered.

CONCLUSION

A geophysical model of earthquake ground motion generation is presented in this paper together with a sensitivity analysis whose purpose is primarily to identify the critical parameters used in the model. It is found that the coherence length and its correlation with the seismic moment as well as the determination of the rise time are the main parameters. It has to be noted that recently several researchers, (including the authors group) have been trying to calculate estimates of coherence lengths by studying actual records, therefore making more reliable the use of this model. However, such a model can be used very simply when not actual but only relative values are necessary. For instance, in the study of bias inherent in a given data collecting network it is planned to use such a model to generate an ensemble of records at simulated or real accelerometers locations. The data will then be analyzed to determine and hopefully correct the bias for the purpose of risk analysis or other earthquake engineering applications.

REFERENCES

(1) Aki, K. (1979), "Characterization of Barriers on an Earthquake Fault," JGR, Vol. 84, No. B11, pp. 6140-6148.

(2) Anderson, J. G. (1976), "Motion Near a Shallow Rupturing Fault: Evaluation of Effects due to the Free Surface," Geophys. J. R. Astr. Soc., 46, pp. 575-593.

(3) Haskell, N. A. (1964), "Total Energy Spectral Density of Elastic Wave Radiation from Propagating Faults(Part I), Bulletin of the Seismological Society of America, Vol. 34, No. 6, pp. 1811-1841.

(4) Haskell, N. A. (1966), "Total Energy Spectral Density of Elastic Wave Radiation from Propagating Faults (Part II), Bulletin of the Seismological Society of America, Vol. 56, No. 1, pp. 125-140.

(5) Savy, J. (1978), "Determination of Seismic Design Parameters, A Stochastic Approach," The John A. Blume Earthquake Center, Stanford, CA., USA, Report No. 34.

(6) Shakal, A. F. (1979), "Analysis and Modelling of the Effects of the Source and Medium on Strong Motion," PhD thesis, MIT, Department of Earth and Planetary Sciences, Cambridge, MA., USA.

(7) Woodward and Clyde Consultants (1979), "Report of the Evaluation of Maximum Earthquake and Site Ground Motion Parameters Associated with the Offshore Zone of Deformation San Onofre Nuclear Generating Station, San Francisco, CA., USA.

S = LxW (kmxkm)	(A) peak accel. a (m/s/s)	(B) τ (sec)	(B) peak accel. a (m/s/s)	(C) ratio τ_2/τ_1	(C) ratio a_2/a_1
6x3	.23	.51	1.16	1/2	2.0
3x1.5	.16	.26	1.51	1/2	1.6
1.5x.75	.10	.13	1.60	1/5	6.7
.6x.3	.03	.05	1.93		

Table I Influences on the single element solution
(A) for various sizes of the element (τ = .25 sec)
(B) for various sizes and rise times combined
(A&B) for seismic moment density kept constant,
(C) for various values of reduction in rise time.

Small earthquake: Seismic moment = 2 10^{17} m.N, S = (6x3) km^2							
Coherence length $\bar{\ell}$ (km)	Peak acceleration a (m/s/s)					average a (m/s/s)	estimated σ_a (m/s/s)
.5	11.35	11.38	6.05	9.85	6.64	9.05	2.56
1.0	5.59	5.70	13.68	5.76	3.47	6.84	3.94
2.0	3.69	4.13	2.14	5.67	2.34	3.59	1.44
3.0	4.89	1.10	1.51	3.44	.90	2.10	1.69
5.0	.47	.59	.65	.87	.44	.61	.17

Medium earthquake: Seismic Moment = 63 10^{17} m.N, S = (19x9.5) km^2		
$\bar{\ell}$	a	
3.0	31.76	(only a single simulation)
6.0	2.23	
9.0	1.55	
15.0	.72	

Table II Effect of variation of the coherence length

S = LxW (kmxkm)	$\bar{\ell}$ (km)	RMS accel. m/s/s
6x3	2	2.26
19x9.5	6	.98
60x30	20	.64

Table III(a) RMS values for different earthquake sizes
site distance = 8km

Distance (km)	RMS accel. m/s/s
6	2.67
8	2.26
12	1.52

Table III (b) RMS values for different site distances and S = (6x3) kmxkm

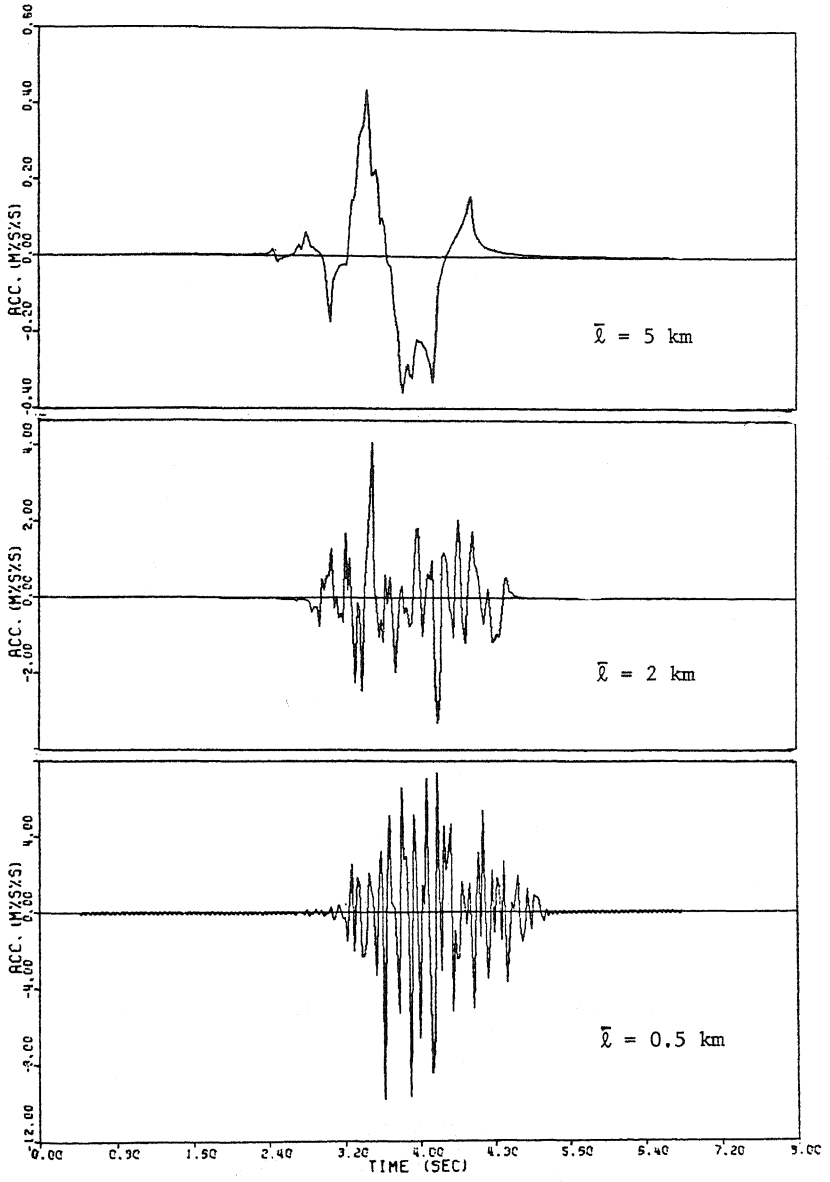

FIGURE I: Evolution of the record shape with coherence length $\bar{\ell}$.

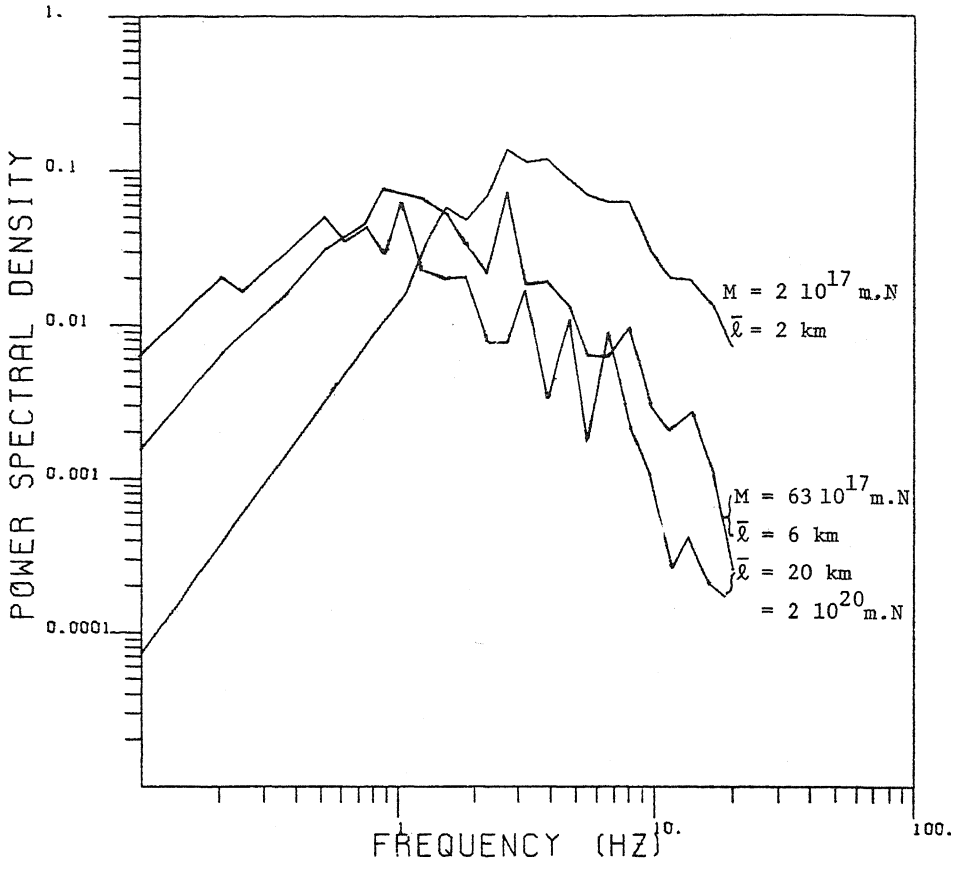

FIGURE II: Power Spectral Density corresponding to three events of increasing seismic moments and increasing coherence length (results of Table III).